ROTATIONAL RAMAN LIDAR FOR TEMPERATURE MEASUREMENTS IN THE TROPOSPHERE

P. A. T. Haris and C. R. Philbrick
Penn State University
Department of Electrical Engineering
University Park, PA 16802
Phone: (814) 863-0851 E-mail: p1h@ecl.psu.edu

Introduction

The use of rotational Raman scattering to measure temperature in the lower troposphere has been investigated. Initial results have shown the value of this technique for temperature measurements from the ground to 10 km using the Applied Research Laboratory/Penn State University LAMP lidar. Comparisons with standard rawinsonde balloons show the rotational Raman technique's accuracy and ability to measure temperature on small spatial and temporal scales. A statistical model of lidar performance, assuming the use of the doubled wavelength (532 nm) Nd:YAG laser, has been developed to analyze the optimal instrumental configuration for rotational Raman temperature measurements in the mid-latitude troposphere.

Pure Rotational Raman Scattering

Pure rotational Raman scattering occurs because of the anisotropic behavior of molecular stretching. As a molecule rotates it stretches due to centripetal forces, causing the molecule to deform. The rotational speed causes the molecules to reside at energy levels above the ground state. If an incident photon excites the rotating molecule to an even higher energy state, the molecule may relax to an energy level which is either greater than (anti-Stoke's region) or less than (Stoke's region) the energy of the incident photon.

The possible energy states, due to rotation, to which a molecule can be excited are quantized. These quantizations are dependent only on temperature. Figure 1 shows the quantum states for the anti-Stoke's branch of the N_2 and O_2 molecule. Figure 2 shows the dependence of the N_2 spectrum on temperature. In a method first proposed by Cooney (1), one could measure temperature by taking the ratio of two measured signals that were received through two filter functions which were placed in the rotational Raman spectrum (Figure 2). The transition from ratio to temperature can be modeled by calculating the response of the rotational Raman spectrum with temperature. The relationship between ratio and temperature is,

$$R(T) = \frac{\sum_S \sum_J (N_S * A_S(J,T) * filtL_S(J)}{\sum_S \sum_J (N_S * A_S(J,T) * filtH_S(J)}$$

where,

$$A(J,T) = \sigma(J)\left[\frac{g(J)}{Q(T)}(2J+1)\exp\left[-1\frac{Bhc}{kT}J(J+1)\right]\right]$$

S	: molecular species
J	: quantum number
N_S	: fraction of species in the atmosphere
filtX(J)	: filter function
σ(J)	: backscatter cross section
g(J)	: nuclear spin statistical weight factor
Q(J)	: rotational partition function
B	: rotational constant

Figure 3 shows the theoretical response curve for the LAMP system. It has been shown that the contribution of pressure broadening on the individual quantum lines is insignificant for normal pressures experienced in the atmosphere (2).

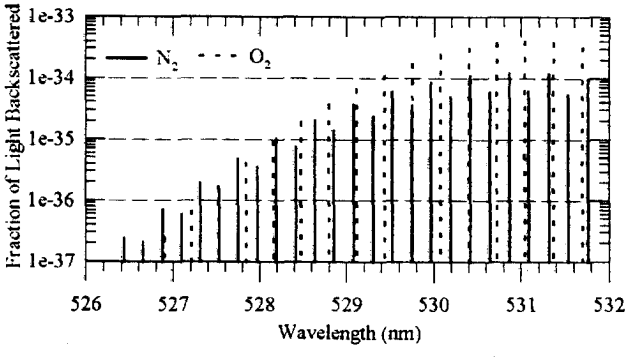

Figure 1: Rotational Raman quantum lines for N_2 and O_2 at 250 K.

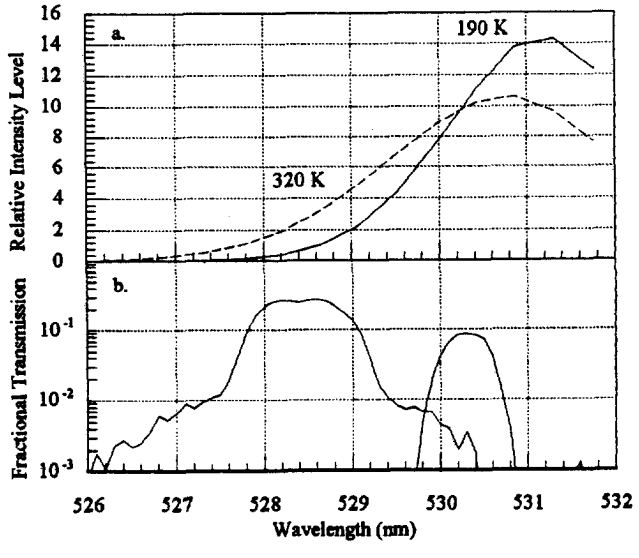

Figure 2a. Temperature dependence of the rotational Raman spectra for N_2 at 190 K and 320 K. 2b. LAMP filter functions used for temperature measurements.

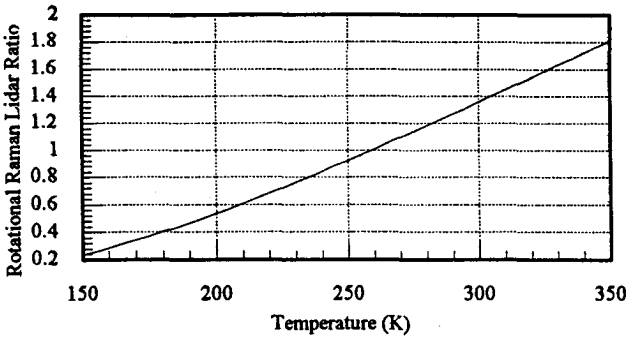

Figure 3. Modeled ratio verses temperature curve for the LAMP lidar.

LAMP Instrument

The construction of the LAMP lidar was completed in the Summer of 1991 at Penn State University. It consists of five primary subsystems: transmitter, receiver, detector, data collector, and safety system (3). The transmitter is a Nd:YAG laser with output wavelengths at 532 nm and 355 nm. The laser operates at 20 Hz emitting 7 nsec long pulses with energies at the two wavelengths of 600 mJ and 250 mJ, respectively. The laser pulses are directed off of three hard coated mirrors before exiting into the atmosphere in a monostatic alignment with the receiver. The backscattered light is directed by an optical flat into a 16" classical Cassigrain telescope. This signal is then directed by a 1 mm diameter fused silica optical fiber into the detector box. The detector box consists of eight separate detector channels (Figure 4) to obtain two wavelengths of elastic scattering data, two wavelengths of vibrational Raman nitrogen and water vapor data, and pure rotational Raman data for determining temperature. The rotational Raman channels have filters placed at 528.4 nm (FWHM = 1.1 nm), and at 530.3 nm (FWHM = 0.6 nm). All channels are set up for photon counting except the elastic scattering channels which use digitizers. The photon counted data is binned with 75m height resolution, while the analog channel is counted into bins with 15 m height resolution. All data channels are averaged in one minute intervals.

LAMP Lidar Measurements

A number of groups have demonstrated the ability of the rotational Raman technique to obtain temperature measurements (4,5,6,7). The technique was installed in the LAMP lidar in 1993 so that high altitude temperature measurements could be extended down to the ground (8). An example of a temperature profiles taken on 07/26/94 at 03:15 UT is shown in Figure 4 along with a radiosonde balloon. The vertical axis represents altitude above sea level. The lidar data begins at the 360 m elevation of State College, PA. The lidar data shows good agreement with the balloon temperatures. The altitude for this profile is limited to only 6 km before the statistical error becomes large. The maximum altitude of the LAMP lidar signal can be increased by allowing more light to fall on the detector. However, this increase in signal in the higher altitudes also causes the signal received from the lower altitudes to become large enough that it saturates the counters in the data collection units and causes a non-linear response. Techniques for removing the non-linearity from the lidar signals are being studied.

Individual lidar profiles can be placed in a time sequence to determine atmospheric movements throughout the course of a night. A preliminary example of this, taken on 09/11/94 between 02:16 - 06:30 UT, is shown in Figure 5, where seven successive 30 minute average lidar profiles have been placed sequentially one after the other. Figure 6 shows a single 30 minute profile taken from Figure 5 which was measured at 03:29 UT. The figures show that the atmosphere in the troposphere was relatively stable. This was consistent with the data from the radiosondes which were launched during the measuring period. Further measurements are to be taken with data averages of 5 - 15 minutes so that small temporal structure may be examined.

The calibration curve to determine the temperature from the lidar data was calculated by performing a least squares fit of the theoretical calibration curve to a second order polynomial of the lidar ratio data verses balloon temperature data.

Instrument Optimization

To measure temperature, using the rotational Raman technique, filter functions in the detector system need to be chosen in order to minimize errors in the lidar data. A program was written to calculate the optimum filter configurations based on filter bandwidth, center wavelength, and minimization of temperature error over a temperature range. The filter functions used in the model were calculated with a modified Gausian function given by,

$$L_{MG}(\omega) = \exp\left[-\left[\frac{(\omega-\omega_o)^2 * \ln 2}{\Delta\omega^2 * \ln 2^{(1-1/x)}}\right]^x\right]$$

where ω is the wave number, ω_o is the center wave number and x is a modifier set equal to 1.4. This function best fit the filter functions which were already installed in the LAMP lidar. Filter functions which did not reduce the fundamental frequency by six orders of magnitude or more were not included in the model. The optimization was calculated to cover the 1% extreme temperatures (190K -320K) from the ground through the tropopause as given by the US Standard Atmosphere 1976. Figure 7 shows the results of the optimization program. The top graph gives the inverse of the relative temperature fractional error that would be obtained given the corresponding filter bandwidths. The values corresponding to the bandwidths are the best values for all choices of filter center wavelengths. The optimal center wavelengths for the bandwidths are given in parts B and C. The algorithm assumes that background counts are negligible compared to the received signal. Thus, the proposed optimum filter configuration is valid only for the dark night time environment. Future calculations will examine the use of the technique for daytime operations.

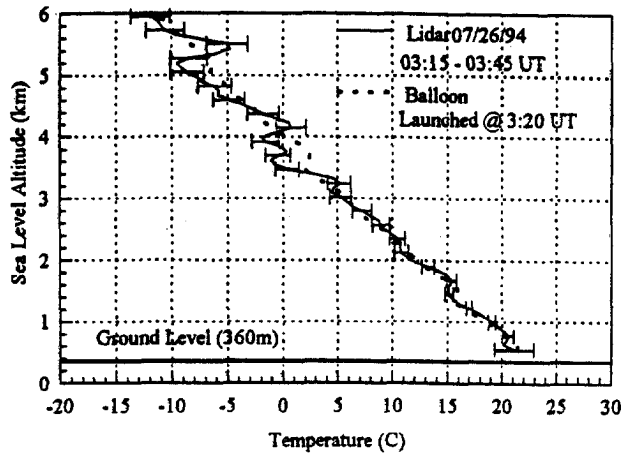

Figure 4. Lidar rotational Raman temperature plot measured on 07/26/94 at 03:15 - 03:45 along with a radiosonde balloon profile. One sigma error bars are based purely on the number of counts received and not on system errors.

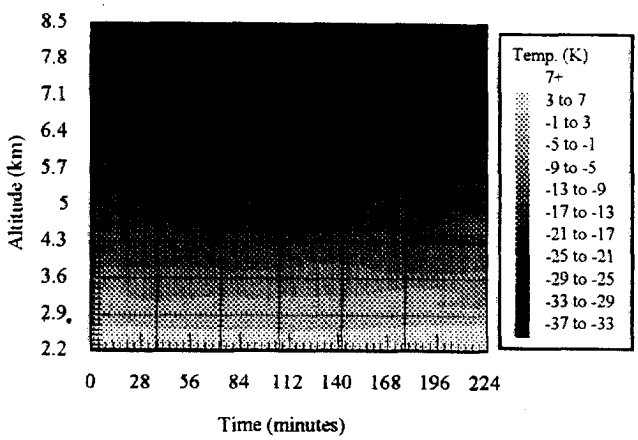

Figure 5. Temperature plot measured on 09/11/94 at 02:16 - 06:30 consisting of seven successive 30 minute average lidar runs. Typical error bars are seen in Figure 6.

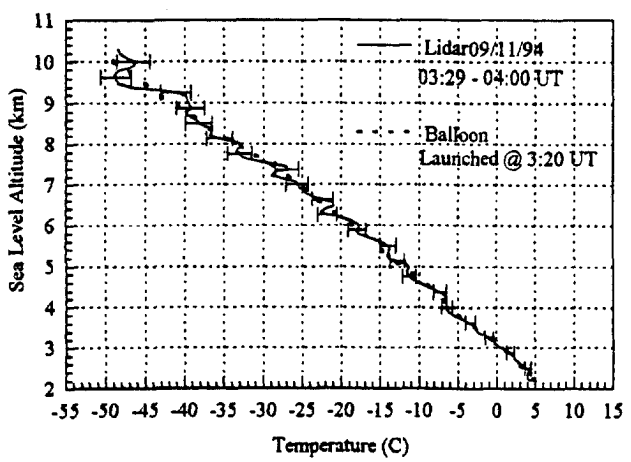

Figure 6. Lidar rotational Raman temperature plot measured on 09/11/94 at 03:29 - 04:00 along with a radiosonde balloon profile. One sigma error bars are based purely on the number of counts received and not on system errors.

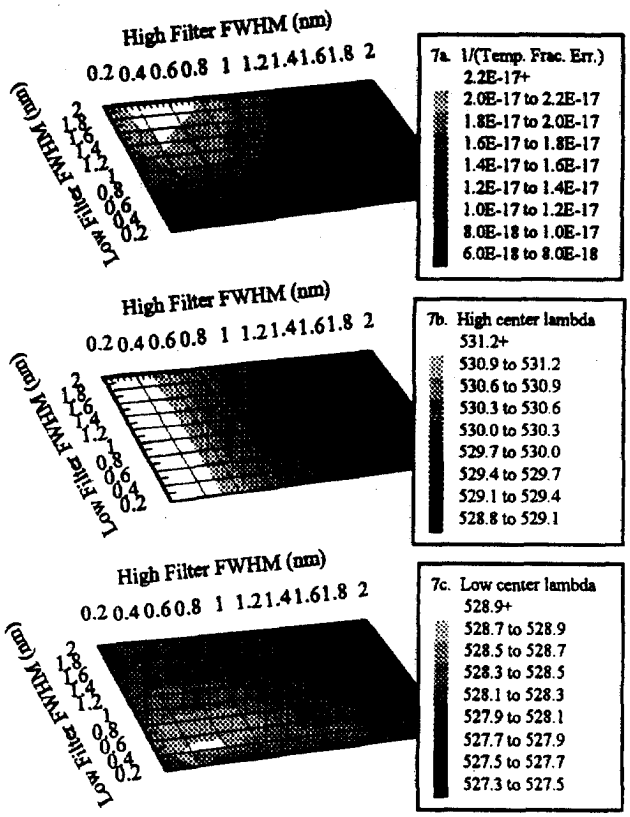

Figure 7. Optimization of filter functions to achieve the lowest statistical error in measuring temperature using the rotational Raman technique. 7a. Best relative inverse temperature statistical errors as a function of filter bandwidth for all filter center wavelengths. Fractional errors do not include system parameters or atmospheric properties except for N_2 and O_2 fractional concentrations. 7b & 7c. Corresponding filter center wavelengths for the values given in 7a.

Acknowledgments

The preparation of the LAMP instrument has been supported by PSU/ARL project initiation funds, PSU College of Engineering, the Navy's Environmental Systems Program Office(SPAWAR PMW-165), and the National Science Foundation's CEDAR (Coupling Energetics and Dynamics of Atmospheric Regions) Program. Thanks are due to Dr. D. Lysak, T. Stevens, S. Rajan, S. Maruvada, S. McKinley, the rest of the Penn State lidar team whose efforts, energies, and time made this paper possible.

References

1. J. A. Cooney, "Measurements of atmospheric temperature profiles by Raman backscatter," J. Appl. Meteorol., Vol 11, pp. 108-112, 1972.
2. D. Nedelijkovic, A. Hauchecorne, and M.-L. Chanin, "Rotational Raman lidar to measure the atmospheric temperature from the ground to 30 km," IEEE Trans. Geosci. Rem. Sens., Vol. 31, pp. 90-101, 1993.

3. T. D. Stevens, "An optical detection system for a Rayleigh /Raman lidar," MS Thesis, Penn State University, 1992.
4. Vaughan, G., D. P. Wareing, S. J. Pepler, L. Thomas, and V. Mitev, "Atmospheric temperature measurements made by rotational Raman scattering," Appl. Opt., Vol. 32, pp. 2758-2764, 1993.
5. A. Cohen, J. A. Cooney, and K. N. Geller, "Atmospheric temperature profiles from lidar measurements of rotational Raman and elastic scattering," Appl. Opt., Vol.15, pp. 2896-2901, 1976.
6. A. Hauchecorne, M.L. Chanin, P. Keckhut, D. Nedeljkovic, "Lidar monitoring of the temperature in the middle and lower atmosphere," Appl. Phys., Vol. B 55, 29-34, 1992.
7. Yu. F. Arshinov, S.M. Bobrovnikov, V.E. Zuev, and V.M. Mitev, "Atmospheric temperature measurements using a pure rotational Raman lidar," Appl. Opt., Vol. 22, pp. 2984-2990, 1983.
8. Philbrick, C.R., "Raman lidar measurements of atmospheric properties," Proceedings of Atmospheric propagation and Remote Sensing III, SPIE 2222, pp.922-931, 1994.